Observation of $e^+e^- \to pp\bar{p}\bar{n}\pi^- + c.c.$*

M. Ablikim (麦迪娜)[1] M. N. Achasov[11,b] P. Adlarson[70] M. Albrecht[4] R. Aliberti[31] A. Amoroso[69A,69C] M. R. An (安美儒)[35] Q. An (安琪)[53,66] X. H. Bai (白旭红)[61] Y. Bai (白羽)[52] O. Bakina[32] R. Baldini Ferroli[26A] I. Balossino[27A,1] Y. Ban (班勇)[42,g] V. Batozskaya[1,40] D. Becker[31] K. Begzsuren[29] N. Berger[31] M. Bertani[26A] D. Bettoni[27A] F. Bianchi[69A,69C] J. Bloms[63] A. Bortone[69A,69C] I. Boyko[32] R. A. Briere[5] A. Brueggemann[63] H. Cai (蔡浩)[71] X. Cai (蔡啸)[1,53] A. Calcaterra[26A] G. F. Cao (曹国富)[1,58] N. Cao (曹宁)[1,58] S. A. Cetin[57A] J. F. Chang (常劲帆)[1,53] W. L. Chang (常万玲)[1,58] G. Chelkov[32,a] C. Chen (陈琛)[39] Chao Chen (陈超)[50] G. Chen (陈刚)[1] H. S. Chen (陈和生)[1,58] M. L. Chen (陈玛丽)[1,53] S. J. Chen (陈申见)[38] S. M. Chen (陈少敏)[56] T. Chen[1] X. R. Chen (陈旭荣)[28,58] X. T. Chen[1] Y. B. Chen (陈元柏)[1,53] Z. J. Chen (陈卓俊)[23,h] W. S. Cheng (成伟帅)[69C] X. Chu (初晓)[39] G. Cibinetto[27A] F. Cossio[69C] J. J. Cui (崔佳佳)[45] H. L. Dai (代洪亮)[1,53] J. P. Dai (代建平)[73] A. Dbeyssi[17] R. E. de Boer[4] D. Dedovich[32] Z. Y. Deng (邓子艳)[1] A. Denig[31] I. Denysenko[32] M. Destefanis[69A,69C] F. De Mori[69A,69C] Y. Ding (丁勇)[36] J. Dong (董静)[1,53] L. Y. Dong (董燎原)[1,58] M. Y. Dong (董明义)[1] X. Dong (董翔)[71] S. X. Du (杜书先)[75] P. Egorov[32,a] Y. L. Fan (范玉兰)[71] J. Fang (方建)[1,53] S. S. Fang (房双世)[1,58] W. X. Fang (方文兴)[1] Y. Fang (方易)[1] R. Farinelli[27A] L. Fava[69B,69C] F. Feldbauer[4] G. Felici[26A] C. Q. Feng (封常青)[53,66] J. H. Feng (冯俊华)[54] K Fischer[64] M. Fritsch[4] C. Fritzsch[63] C. D. Fu (傅成栋)[1] H. Gao (高涵)[58] Y. N. Gao (高原宁)[42,g] Yang Gao (高扬)[53,66] S. Garbolino[69C] I. Garzia[27A,27B] P. T. Ge (葛潘婷)[71] Z. W. Ge (葛振武)[38] C. Geng (耿聪)[54] E. M. Gersabeck[62] A Gilman[64] K. Goetzen[12] L. Gong (龚丽)[36] W. X. Gong (龚文煊)[1,53] W. Gradl[31] M. Greco[69A,69C] L. M. Gu (谷立民)[38] M. H. Gu (顾旻皓)[1,53] Y. T. Gu (顾运厅)[14] C. Y. Guan (关春懿)[1,58] A. Q. Guo (郭爱强)[28,58] L. B. Guo (郭立波)[37] R. P. Guo (郭如盼)[44] Y. P. Guo (郭玉萍)[10,f] A. Guskov[32,a] T. T. Han (韩婷婷)[45] W. Y. Han (韩文颖)[35] X. Q. Hao (郝喜庆)[18] F. A. Harris[60] K. K. He (何凯凯)[50] K. L. He (何康林)[1,58] F. H. Heinsius[4] C. H. Heinz[31] Y. K. Heng (衡月昆)[1] C. Herold[55] M. Himmelreich[12,d] G. Y. Hou (侯国一)[1,58] Y. R. Hou (侯颖锐)[58] Z. L. Hou (侯治龙)[1] H. M. Hu (胡海明)[1,58] J. F. Hu[51,i] T. Hu (胡涛)[1] Y. Hu (胡誉)[1] G. S. Huang (黄光顺)[53,66] K. X. Huang (黄凯旋)[54] L. Q. Huang (黄麟钦)[67] L. Q. Huang (黄麟钦)[28,58] X. T. Huang (黄性涛)[45] Y. P. Huang (黄燕萍)[1] Z. Huang (黄震)[42,g] T. Hussain[68] N Hüsken[25,31] W. Imoehl[25] M. Irshad[53,66] J. Jackson[25] S. Jaeger[4] S. Janchiv[29] Q. Ji (纪全)[1] Q. P. Ji (姬清平)[18] X. B. Ji (季晓斌)[1,58] X. L. Ji (季筱璐)[1,53] Y. Y. Ji (吉钰瑶)[45] Z. K. Jia (贾泽坤)[53,66] H. B. Jiang (姜侯兵)[45] S. S. Jiang (姜赛赛)[35] X. S. Jiang (江晓山)[1] Y. Jiang[58] J. B. Jiao (焦健斌)[45] Z. Jiao (焦铮)[21] S. Jin (金山)[38] Y. Jin (金毅)[61] M. Q. Jing (荆茂强)[1,58] T. Johansson[70] N. Kalantar-Nayestanaki[59] X. S. Kang (康晓珅)[36] R. Kappert[59] B. C. Ke (柯百谦)[75] I. K. Keshk[4] A. Khoukaz[63] P. Kiese[31] R. Kiuchi[1] R. Kliemt[12] L. Koch[33] O. B. Kolcu[57A] B. Kopf[4] M. Kuemmel[4] M. Kuessner[4] A. Kupsc[40,70] W. Kühn[33]

Received 25 November 2022; Accepted 30 January 2023; Published online 1 February 2023

* Supported in part by National Key R&D Program of China under Contracts Nos. Supported in part by National Key R&D Program of China (2020YFA0406300, 2020YFA0406400); National Natural Science Foundation of China (NSFC) (11975118, 11625523, 11635010, 11735014, 11822506, 11835012, 11935015, 11935016, 11935018, 11961141012, 12022510, 12025502, 12035009, 12035013, 12061131003, 12075252, 12192260, 12192261, 12192262, 12192263, 12192264, 12192265); the Natural Science Foundation of Hunan Province of China (2019JJ30019); the Science and Technology Innovation Program of Hunan Province (2020RC3054); the Chinese Academy of Sciences (CAS) Large-Scale Scientific Facility Program; Joint Large-Scale Scientific Facility Funds of the NSFC and CAS (U1732263, U1832207); CAS Key Research Program of Frontier Sciences (QYZDJ-SSW-SLH040); 100 Talents Program of CAS; INPAC and Shanghai Key Laboratory for Particle Physics and Cosmology; ERC (758462); European Union Horizon 2020 research and innovation programme under Contract No. Marie Sklodowska-Curie grant agreement (894790); German Research Foundation DFG (43159800), Collaborative Research Center CRC 1044, FOR 2359, GRK 2149; Istituto Nazionale di Fisica Nucleare, Italy; Ministry of Development of Turkey (DPT2006K-120470); National Science and Technology fund; Olle Engkvist Foundation (200-0605); STFC (United Kingdom); The Knut and Alice Wallenberg Foundation (Sweden) (2016.0157); The Royal Society, UK (DH140054, DH160214); The Swedish Research Council; U. S. Department of Energy (DE-FG02-05ER41374, DE-SC-0012069)

J. J. Lane[62] J. S. Lange[33] P. Larin[17] A. Lavania[24] L. Lavezzi[69A,69C] Z. H. Lei (雷祚弘)[53,66] H. Leithoff[31]
M. Lellmann[31] T. Lenz[31] C. Li (李翠)[43] C. Li (李聪)[39] C. H. Li (李春花)[35] Cheng Li (李澄)[53,66]
D. M. Li (李德民)[75] F. Li (李飞)[1,53] G. Li (李刚)[1] H. Li (李慧)[47] H. Li (李贺)[53,66] H. B. Li (李海波)[1,58]
H. J. Li (李惠静)[18] H. N. Li[51,i] J. Q. Li[4] J. S. Li (李静舒)[54] J. W. Li (李井文)[45] Ke Li (李科)[1] L. J. Li[1]
L. K. Li (李龙科)[1] Lei Li (李蕾)[3] M. H. Li (李明浩)[39] P. R. Li (李培荣)[34,j,k] S. X. Li (李素娴)[10]
S. Y. Li (栗帅迎)[56] T. Li (李腾)[45] W. D. Li (李卫东)[1,58] W. G. Li (李卫国)[1] X. H. Li (李旭红)[53,66]
X. L. Li (李晓玲)[45] Xiaoyu Li (李晓宇)[1,58] H. Liang (梁昊)[53,66] H. Liang (梁浩)[1,58] H. Liang (梁浩)[30]
Y. F. Liang (梁勇飞)[49] Y. T. Liang (梁羽铁)[28,58] G. R. Liao (廖广睿)[13] L. Z. Liao (廖龙洲)[45] J. Libby[24]
A. Limphirat[55] C. X. Lin (林创新)[54] D. X. Lin (林德旭)[28,58] T. Lin[1] B. J. Liu (刘北江)[1] C. X. Liu (刘春秀)[1]
D. Liu[17,66] F. H. Liu (刘福虎)[48] Fang Liu (刘芳)[1] Feng Liu (刘峰)[6] G. M. Liu[51,i] H. Liu[34,j,k]
H. B. Liu (刘宏邦)[14] H. M. Liu (刘怀民)[1,58] Huanhuan Liu (刘欢欢)[1] Huihui Liu (刘汇慧)[19] J. B. Liu (刘建北)[53,66]
J. L. Liu (刘佳俊)[67] J. Y. Liu (刘晶译)[1,58] K. Liu (刘凯)[1] K. Y. Liu (刘魁勇)[36] Ke Liu (刘珂)[20]
L. Liu (刘亮)[53,66] Lu Liu (刘露)[39] M. H. Liu (刘美宏)[10,f] P. L. Liu (刘佩莲)[1] Q. Liu (刘倩)[58]
S. B. Liu (刘树彬)[53,66] T. Liu (刘桐)[10,f] W. K. Liu (刘维克)[39] W. M. Liu (刘卫民)[53,66] X. Liu (刘翔)[34,j,k]
Y. Liu (刘英)[34,j,k] Y. B. Liu (刘玉斌)[39] Z. A. Liu (刘振安)[1] Z. Q. Liu (刘智青)[45] X. C. Lou (娄辛丑)[1]
F. X. Lu (卢飞翔)[54] H. J. Lu (吕海江)[21] J. G. Lu (吕军光)[1,53] X. L. Lu (陆小玲)[1] Y. Lu (卢宇)[7]
Y. P. Lu (卢云鹏)[1,53] Z. H. Lu[1] C. L. Luo (罗成林)[37] M. X. Luo (罗民兴)[74] T. Luo (罗涛)[10,f]
X. L. Luo (罗小兰)[1,53] X. R. Lyu (吕晓睿)[58] Y. F. Lyu (吕翌丰)[39] F. C. Ma (马凤才)[36] H. L. Ma (马海龙)[1]
L. L. Ma (马连良)[45] M. M. Ma (马明明)[1,58] Q. M. Ma (马秋梅)[1] R. Q. Ma (马润秋)[1,58] R. T. Ma (马瑞廷)[58]
X. Y. Ma (马骁妍)[1,53] Y. Ma (马尧)[42,g] F. E. Maas[17] M. Maggiora[69A,69C] S. Maldaner[4] S. Malde[64]
Q. A. Malik[68] A. Mangoni[26B] Y. J. Mao (冒亚军)[42,g] Z. P. Mao (毛泽普)[1] S. Marcello[69A,69C]
Z. X. Meng (孟召霞)[61] J. G. Messchendorp[59] G. Mezzadri[27A,1] H. Miao[1] T. J. Min (闵天觉)[38] R. E. Mitchell[25]
X. H. Mo (莫晓虎)[1] N. Yu. Muchnoi[11,b] Y. Nefedov[32] F. Nerling[17,d] I. B. Nikolaev[11,b] Z. Ning (宁哲)[1,53]
S. Nisar[9,l] Y. Niu (牛艳)[45] S. L. Olsen[58] Q. Ouyang (欧阳群)[1] S. Pacetti[26B,26C] X. Pan (潘祥)[10,f]
Y. Pan (潘越)[52] A. Pathak[30] M. Pelizaeus[4] H. P. Peng (彭海平)[53,66] K. Peters[12,d] J. L. Ping (平加伦)[37]
R. G. Ping (平荣刚)[1,58] S. Plura[31] S. Pogodin[32] V. Prasad[53,66] F. Z. Qi (齐法制)[1] H. Qi (齐航)[53,66]
H. R. Qi (漆红荣)[56] M. Qi (祁鸣)[38] T. Y. Qi (齐天钰)[10,f] S. Qian (钱森)[1,53] W. B. Qian (钱文斌)[58]
Z. Qian (钱圳)[54] C. F. Qiao (乔从丰)[58] J. J. Qin (秦佳佳)[67] L. Q. Qin (秦丽清)[13] X. P. Qin (覃潇平)[10,f]
X. S. Qin (秦小帅)[45] Z. H. Qin (秦中华)[1,53] J. F. Qiu (邱进发)[1] S. Q. Qu (屈三强)[56] K. H. Rashid[68]
C. F. Redmer[31] K. J. Ren (任旷洁)[35] A. Rivetti[69C] V. Rodin[59] M. Rolo[69C] G. Rong (荣刚)[1,58] Ch. Rosner[17]
S. N. Ruan (阮氏宁)[39] H. S. Sang (桑昊榆)[66] A. Sarantsev[32,c] Y. Schelhaas[31] C. Schnier[4] K. Schoenning[70]
M. Scodeggio[27A,27B] K. Y. Shan (尚科羽)[10,f] W. Shan (单葳)[22] X. Y. Shan (单心钰)[53,66]
J. F. Shangguan (上官剑锋)[50] L. G. Shao (邵立港)[1,58] M. Shao (邵明)[53,66] C. P. Shen (沈成平)[10,f]
H. F. Shen (沈宏飞)[1,58] X. Y. Shen (沈肖雁)[1,58] B. A. Shi (施伯安)[58] H. C. Shi (石煌超)[53,66] J. Y. Shi (石京燕)[1]
Q. Q. Shi (石勤强)[50] R. S. Shi (师荣盛)[1,58] X. Shi (史欣)[1,53] X. D Shi (师晓东)[53,66] J. J. Song (宋娇娇)[18]
W. M. Song (宋维民)[1,30] Y. X. Song (宋昀轩)[42,g] S. Sosio[69A,69C] S. Spataro[69A,69C] F. Stieler[31] K. X. Su (苏可馨)[71]
P. P. Su (苏彭彭)[50] Y. J. Su (粟杨捷)[58] G. X. Sun (孙功星)[1] H. Sun[58] H. K. Sun (孙浩凯)[1]
J. F. Sun (孙俊峰)[18] L. Sun (孙亮)[71] S. S. Sun (孙胜森)[1,58] T. Sun (孙童)[1,58] W. Y. Sun (孙文玉)[30]
X Sun (孙翔)[23,h] Y. J. Sun (孙勇杰)[53,66] Y. Z. Sun (孙永昭)[1] Z. T. Sun (孙振田)[45] Y. H. Tan (谭英华)[71]
Y. X. Tan (谭雅星)[53,66] C. J. Tang (唐昌建)[49] G. Y. Tang (唐光毅)[1] J. Tang (唐健)[54] L. Y. Tao (陶璐燕)[67]
Q. T. Tao (陶秋田)[23,h] M. Tat[64] J. X. Teng (滕佳秀)[53,66] V. Thoren[70] W. H. Tian (田文辉)[47] Y. Tian (田野)[28,58]
I. Uman[57B] B. Wang (王斌)[1] B. L. Wang (王滨龙)[58] C. W. Wang (王成伟)[38] D. Y. Wang (王大勇)[42,g]
F. Wang (王菲)[67] H. J. Wang (王泓鉴)[34,j,k] H. P. Wang (王宏鹏)[1,58] K. Wang (王科)[1,53] L. L. Wang (王亮亮)[1]
M. Wang (王萌)[45] M. Z. Wang (王梦真)[42,g] Meng Wang (王蒙)[1,58] S. Wang[13] S. Wang (王顺)[10,f]
T. Wang (王婷)[10,f] T. J. Wang (王腾蛟)[39] W. Wang (王为)[54] W. H. Wang (王文欢)[71] W. P. Wang (王维平)[53,66]
X. Wang (王轩)[42,g] X. F. Wang (王雄飞)[34,j,k] X. L. Wang (王小龙)[10,f] Y. Wang (王亦)[56] Y. D. Wang (王雅迪)[41]

Y. F. Wang (王贻芳)[1] Y. H. Wang (王英豪)[43] Y. Q. Wang (王雨晴)[1] Yaqian Wang (王亚乾)[1,16]
Z. Wang (王铮)[1,53] Z. Y. Wang (王至勇)[1,58] Ziyi Wang (王子一)[58] D. H. Wei (魏代会)[13] F. Weidner[63]
S. P. Wen (文硕频)[1] D. J. White[62] U. Wiedner[4] G. Wilkinson[64] M. Wolke[70] L. Wollenberg[4]
J. F. Wu (吴金飞)[1,58] L. H. Wu (伍灵慧)[1] L. J. Wu (吴连近)[1,58] X. Wu (吴潇)[10,f] X. H. Wu (伍雄浩)[30]
Y. Wu[66] Z. Wu (吴智)[1,53] L. Xia (夏磊)[53,66] T. Xiang (相腾)[42,g] D. Xiao (肖栋)[34,j,k] G. Y. Xiao (肖光延)[38]
H. Xiao (肖浩)[10,f] S. Y. Xiao (肖素玉)[1] Y. L. Xiao (肖云龙)[10,f] Z. J. Xiao (肖振军)[37] C. Xie (谢陈)[38]
X. H. Xie (谢昕海)[42,g] Y. Xie (谢勇)[45] Y. G. Xie (谢宇广)[1,53] Y. H. Xie (谢跃红)[6] Z. P. Xie (谢智鹏)[53,66]
T. Y. Xing (邢天宇)[1,58] C. F. Xu[1] C. J. Xu (许创杰)[54] G. F. Xu (许国发)[1] H. Y. Xu (许皓月)[61]
Q. J. Xu (徐庆君)[15] X. P. Xu (徐新平)[50] Y. C. Xu (胥英超)[58] Z. P. Xu (许泽鹏)[38] F. Yan (严芳)[10,f]
L. Yan (严亮)[10,f] W. B. Yan (鄢文标)[53,66] W. C. Yan (闫文成)[75] H. J. Yang (杨海军)[46,e] H. L. Yang (杨昊霖)[30]
H. X. Yang (杨洪勋)[1] L. Yang (杨玲)[47] S. L. Yang[58] Tao Yang (杨涛)[1] Y. F. Yang (杨艳芳)[39]
Y. X. Yang (杨逸翔)[1,58] Yifan Yang (杨翊凡)[1,58] M. Ye (叶梅)[1,53] M. H. Ye (叶铭汉)[8] J. H. Yin (殷俊昊)[1]
Z. Y. You (尤郑昀)[54] B. X. Yu (俞伯祥)[1] C. X. Yu (喻纯旭)[39] G. Yu (余刚)[1,58] T. Yu (于涛)[67]
C. Z. Yuan (苑长征)[1,58] L. Yuan (袁丽)[2] S. C. Yuan[1] X. Q. Yuan (袁晓庆)[1] Y. Yuan (袁野)[1,58]
Z. Y. Yuan (袁朝阳)[54] C. X. Yue (岳崇兴)[35] A. A. Zafar[68] F. R. Zeng (曾凡蕊)[45] X. Zeng (曾鑫)[6]
Y. Zeng (曾云)[23,h] Y. H. Zhan (詹永华)[54] A. Q. Zhang (张安庆)[1] B. L. Zhang[1] B. X. Zhang (张丙新)[1]
D. H. Zhang (张丹昊)[39] G. Y. Zhang (张广义)[18] H. Zhang[66] H. H. Zhang (张宏浩)[54] H. H. Zhang (张宏宏)[30]
H. Y. Zhang (章红宇)[1,53] J. L. Zhang (张杰磊)[72] J. Q. Zhang (张敬庆)[37] J. W. Zhang (张家文)[1] J. X. Zhang[34,j,k]
J. Y. Zhang (张建勇)[1] J. Z. Zhang (张景芝)[1,58] Jianyu Zhang (张剑宇)[1,58] Jiawei Zhang (张嘉伟)[1,58]
L. M. Zhang (张黎明)[56] L. Q. Zhang (张丽青)[54] Lei Zhang (张雷)[38] P. Zhang[1] Q. Y. Zhang (张秋岩)[35,75]
Shuihan Zhang (张水涵)[1,58] Shulei Zhang (张书磊)[23,h] X. D. Zhang (张小东)[41] X. M. Zhang[1]
X. Y. Zhang (张学尧)[45] X. Y. Zhang (张旭颜)[50] Y. Zhang[64] Y. T. Zhang (张亚腾)[75] Y. H. Zhang (张银鸿)[1,53]
Yan Zhang (张言)[53,66] Yao Zhang (张瑶)[1] Z. H. Zhang[1] Z. Y. Zhang (张振宇)[71] Z. Y. Zhang (张子羽)[39]
G. Zhao (赵光)[1] J. Zhao (赵静)[35] J. Y. Zhao (赵静宜)[1,58] J. Z. Zhao (赵京周)[1,53] Lei Zhao (赵雷)[53,66]
Ling Zhao (赵玲)[1] M. G. Zhao (赵明刚)[39] Q. Zhao (赵强)[1] S. J. Zhao (赵书俊)[75] Y. B. Zhao (赵豫斌)[1,53]
Y. X. Zhao (赵宇翔)[28,58] Z. G. Zhao (赵政国)[53,66] A. Zhemchugov[32,a] B. Zheng (郑波)[67] J. P. Zheng (郑建平)[1,53]
Y. H. Zheng (郑阳恒)[58] B. Zhong (钟彬)[37] C. Zhong (钟翠)[67] X. Zhong (钟鑫)[54] H. Zhou (周航)[45]
L. P. Zhou (周利鹏)[1,58] X. Zhou (周详)[71] X. K. Zhou (周晓康)[58] X. R. Zhou (周小蓉)[53,66] X. Y. Zhou (周兴玉)[35]
Y. Z. Zhou (周祎卓)[10,f] J. Zhu (朱江)[39] K. Zhu (朱凯)[1] K. J. Zhu (朱科军)[1] L. X. Zhu (朱琳萱)[58]
S. H. Zhu (朱世海)[65] S. Q. Zhu (朱仕强)[38] T. J. Zhu (朱腾蛟)[72] W. J. Zhu (朱文静)[10,f] Y. C. Zhu (朱莹春)[53,66]
Z. A. Zhu (朱自安)[1,58] B. S. Zou (邹冰松)[1] J. H. Zou (邹佳恒)[1]

(BESIII Collaboration)

[1]Institute of High Energy Physics, Beijing 100049, China
[2]Beihang University, Beijing 100191, China
[3]Beijing Institute of Petrochemical Technology, Beijing 102617, China
[4]Bochum Ruhr-University, D-44780 Bochum, Germany
[5]Carnegie Mellon University, Pittsburgh, Pennsylvania 15213, USA
[6]Central China Normal University, Wuhan 430079, China
[7]Central South University, Changsha 410083, China
[8]China Center of Advanced Science and Technology, Beijing 100190, China
[9]COMSATS University Islamabad, Lahore Campus, Defence Road, Off Raiwind Road, 54000 Lahore, Pakistan
[10]Fudan University, Shanghai 200433, China
[11]G.I. Budker Institute of Nuclear Physics SB RAS (BINP), Novosibirsk 630090, Russia
[12]GSI Helmholtzcentre for Heavy Ion Research GmbH, D-64291 Darmstadt, Germany
[13]Guangxi Normal University, Guilin 541004, China
[14]Guangxi University, Nanning 530004, China
[15]Hangzhou Normal University, Hangzhou 310036, China
[16]Hebei University, Baoding 071002, China
[17]Helmholtz Institute Mainz, Staudinger Weg 18, D-55099 Mainz, Germany
[18]Henan Normal University, Xinxiang 453007, China
[19]Henan University of Science and Technology, Luoyang 471003, China
[20]Henan University of Technology, Zhengzhou 450001, China
[21]Huangshan College, Huangshan 245000, China

[22]Hunan Normal University, Changsha 410081, China
[23]Hunan University, Changsha 410082, China
[24]Indian Institute of Technology Madras, Chennai 600036, India
[25]Indiana University, Bloomington, Indiana 47405, USA
[26A]INFN Laboratori Nazionali di Frascati, I-00044, Frascati, Italy
[26B]INFN Sezione di Perugia, I-06100, Perugia, Italy
[26C]University of Perugia, I-06100, Perugia, Italy
[27A]INFN Sezione di Ferrara, I-44122, Ferrara, Italy
[27B]University of Ferrara, I-44122, Ferrara, Italy
[28]Institute of Modern Physics, Lanzhou 730000, China
[29]Institute of Physics and Technology, Peace Avenue 54B, Ulaanbaatar 13330, Mongolia
[30]Jilin University, Changchun 130012, China
[31]Johannes Gutenberg University of Mainz, Johann-Joachim-Becher-Weg 45, D-55099 Mainz, Germany
[32]Joint Institute for Nuclear Research, 141980 Dubna, Moscow region, Russia
[33]Justus-Liebig-Universitaet Giessen, II. Physikalisches Institut, Heinrich-Buff-Ring 16, D-35392 Giessen, Germany
[34]Lanzhou University, Lanzhou 730000, China
[35]Liaoning Normal University, Dalian 116029, China
[36]Liaoning University, Shenyang 110036, China
[37]Nanjing Normal University, Nanjing 210023, China
[38]Nanjing University, Nanjing 210093, China
[39]Nankai University, Tianjin 300071, China
[40]National Centre for Nuclear Research, Warsaw 02-093, Poland
[41]North China Electric Power University, Beijing 102206, China
[42]Peking University, Beijing 100871, China
[43]Qufu Normal University, Qufu 273165, China
[44]Shandong Normal University, Jinan 250014, China
[45]Shandong University, Jinan 250100, China
[46]Shanghai Jiao Tong University, Shanghai 200240, China
[47]Shanxi Normal University, Linfen 041004, China
[48]Shanxi University, Taiyuan 030006, China
[49]Sichuan University, Chengdu 610064, China
[50]Soochow University, Suzhou 215006, China
[51]South China Normal University, Guangzhou 510006, China
[52]Southeast University, Nanjing 211100, China
[53]State Key Laboratory of Particle Detection and Electronics, Beijing 100049, Hefei 230026, China
[54]Sun Yat-Sen University, Guangzhou 510275, China
[55]Suranaree University of Technology, University Avenue 111, Nakhon Ratchasima 30000, Thailand
[56]Tsinghua University, Beijing 100084, China
[57A]Istinye University, 34010, Istanbul, Turkey
[57B]Near East University, Nicosia, North Cyprus, Mersin 10, Turkey
[58]University of Chinese Academy of Sciences, Beijing 100049, China
[59]University of Groningen, NL-9747 AA Groningen, The Netherlands
[60]University of Hawaii, Honolulu, Hawaii 96822, USA
[61]University of Jinan, Jinan 250022, China
[62]University of Manchester, Oxford Road, Manchester, M13 9PL, United Kingdom
[63]University of Muenster, Wilhelm-Klemm-Strasse 9, 48149 Muenster, Germany
[64]University of Oxford, Keble Road, Oxford OX13RH, United Kingdom
[65]University of Science and Technology Liaoning, Anshan 114051, China
[66]University of Science and Technology of China, Hefei 230026, China
[67]University of South China, Hengyang 421001, China
[68]University of the Punjab, Lahore-54590, Pakistan
[69A]University of Turin, I-10125, Turin, Italy
[69B]University of Eastern Piedmont, I-15121, Alessandria, Italy
[69C]INFN, I-10125, Turin, Italy
[70]Uppsala University, Box 516, SE-75120 Uppsala, Sweden
[71]Wuhan University, Wuhan 430072, China
[72]Xinyang Normal University, Xinyang 464000, China
[73]Yunnan University, Kunming 650500, China
[74]Zhejiang University, Hangzhou 310027, China
[75]Zhengzhou University, Zhengzhou 450001, China
[a]Also at the Moscow Institute of Physics and Technology, Moscow 141700, Russia
[b]Also at the Novosibirsk State University, Novosibirsk, 630090, Russia
[c]Also at the NRC "Kurchatov Institute", PNPI, 188300, Gatchina, Russia
[d]Also at Goethe University Frankfurt, 60323 Frankfurt am Main, Germany
[e]Also at Key Laboratory for Particle Physics, Astrophysics and Cosmology, Ministry of Education; Shanghai Key Laboratory for Particle Physics and Cosmology; Institute of Nuclear and Particle Physics, Shanghai 200240, China
[f]Also at Key Laboratory of Nuclear Physics and Ion-beam Application (MOE) and Institute of Modern Physics, Fudan University, Shanghai 200443, China

[g]Also at State Key Laboratory of Nuclear Physics and Technology, Peking University, Beijing 100871, China
[h]Also at School of Physics and Electronics, Hunan University, Changsha 410082, China
[i]Also at Guangdong Provincial Key Laboratory of Nuclear Science, Institute of Quantum Matter, South China Normal University, Guangzhou 510006, China
[j]Also at Frontiers Science Center for Rare Isotopes, Lanzhou University, Lanzhou 730000, China
[k]Also at Lanzhou Center for Theoretical Physics, Lanzhou University, Lanzhou 730000, China
[l]Also at the Department of Mathematical Sciences, IBA, Karachi, Pakistan

Abstract: Using data taken at 29 center-of-mass energies between 4.16 and 4.70 GeV with the BESIII detector at the Beijing Electron Positron Collider corresponding to a total integrated luminosity of approximately 18.8 fb^{-1}, the process $e^+e^- \to p p\bar{p}\bar{n}\pi^- + c.c.$ is observed for the first time with a statistical significance of 11.5σ. The average Born cross sections in the energy ranges of (4.160, 4.380) GeV, (4.400, 4.600) GeV and (4.610, 4.700) GeV are measured to be $(21.5 \pm 5.7 \pm 1.2)$ fb, $(46.3 \pm 10.6 \pm 2.5)$ fb and $(59.0 \pm 9.4 \pm 3.2)$ fb, respectively, where the first uncertainties are statistical and the second are systematic. The line shapes of the $\bar{p}\bar{n}$ and $pp\pi^-$ invariant mass spectra are consistent with phase space distributions, indicating that no hexaquark or di-baryon state is observed.

Keywords: Multi-baryon channel, hexaquark, di-baryon states, cross section measurement

DOI: 10.1088/1674-1137/acb6eb

I. INTRODUCTION

One of the most fundamental questions in hadron physics is related to the mechanism of color confinement in Quantum Chromodynamics (QCD). Color-singlet hadronic configurations of quarks and gluons can form bound states or resonances. Besides the well-known combinations of $q\bar{q}$ for mesons and qqq for baryons, other combinations, such as $gq\bar{q}$ for hybrid states [1], multi-gluons for glueball states [2], $q\bar{q}q\bar{q}$ for tetraquark states [3], $qqqq\bar{q}$ for pentaquark states [4] and hexaquark states ($qqqqqq$) [5], are also allowed by QCD. Di-baryon [6] and hexaquark states have been searched for in a range of nucleon-nucleon scattering reactions. Recently, an isoscalar resonant structure was observed in the isoscalar two-pionic fusion process $pn \to d\pi^0\pi^0$ [7] by the WASA Collaboration and was later confirmed in the other two-pionic fusion processes $pn \to d\pi^+\pi^-$ [8] and $pp \to d\pi^+\pi^0$ [9], and the two-pionic non-fusion process $pn \to pp\pi^0\pi^-$ [10] and $pn \to pn\pi^0\pi^0$ [11]. This state was denoted by $d^*(2380)$ following the convention used for nucleon excitations. These observations indicate the possibility of the existence of hexaquark and di-baryon configurations. In 2021, the BESIII Collaboration reported the search for hexaquark and di-baryon states in examining the invariant mass spectra of two baryons in the process $e^+e^- \to 2(p\bar{p})$ [12], and no significant signal was observed.

Analyzing data sets corresponding to a total integrated luminosity of approximately 18.8 fb^{-1} taken at center-of-mass energies $\sqrt{s}$ between 4.16 and 4.70 GeV with the BESIII detector, we present in this paper the first measurement of the cross section of the process $e^+e^- \to p p\bar{p}\bar{n}\pi^- + c.c.$. We search for the $d^*(2380)$ and other possible hexaquark or di-baryon states with the data samples with energies above 4.60 GeV, where the $\bar{p}\bar{n}$ system with a mass around 2.4 GeV for $d^*(2380)$ is kinematically accessible. The mass range of the $\bar{p}\bar{n}$ system around 2.4 GeV/c^2, in which the $d^*(2380)$ might contribute, is covered by the data samples with energies above 4.60 GeV. Throughout this paper, charge conjugation is always implied unless explicitly stated, and in discussing systematic uncertainties.

II. THE BESIII DETECTOR AND DATA SAMPLES

The BESIII detector [13] records symmetric e^+e^- collisions provided by the BEPCII storage ring [14], which operates in the center-of-mass energy range from 2.0 to 4.95 GeV. BESIII has collected large data samples in this energy region [15]. The cylindrical core of the BESIII detector covers 93% of the full solid angle and consists of a helium-based multilayer drift chamber (MDC), a plastic scintillator time-of-flight system (TOF), and a CsI(Tl) electromagnetic calorimeter (EMC), which are all enclosed in a superconducting solenoidal magnet providing a 1.0 T magnetic field. The solenoid is supported by an octagonal flux-return yoke with resistive plate counter muon identification modules interleaved with steel. The charged-particle momentum resolution at 1 GeV/c is 0.5%, and the specific energy loss (dE/dx) resolution is 6% for electrons from Bhabha scattering. The EMC measures photon energies with a resolution of 2.5% (5%) at 1 GeV in the barrel (end cap) region. The time resolution in the TOF barrel region is 68 ps, while that in the end cap region is 110 ps. The end cap TOF system was upgraded in 2015 using multi-gap resistive plate chamber technology, providing a time resolution of 60 ps [16, 17].

The data sets were collected at 29 center-of-mass energies between 4.16 and 4.70 GeV. The nominal energies of the data sets from 4.16 to 4.60 GeV are measured by

the di-muon process $e^+e^- \to (\gamma_{\rm ISR/FSR})\mu^+\mu^-$ [18, 19], where the subscript ISR/FSR stands for the initial-state or final-state radiation process, respectively. Those for the data sets from 4.61 to 4.70 GeV are calibrated by the process $e^+e^- \to \Lambda_c^+\bar{\Lambda}_c^-$ [20]. The integrated luminosity $\mathcal{L}_{\rm int}$ is determined using large-angle Bhabha scattering events [20, 21]. The total integrated luminosity of all data sets is approximately 18.8 fb^{-1}.

The response of the BESIII detector is modeled with Monte Carlo (MC) simulations using the software framework BOOST [22] based on geant4 [23], which includes the geometry and material description of the BESIII detector, the detector response and digitization models, as well as a database that keeps track of the running conditions and the detector performance. Large MC simulated event samples are used to optimize the selection criteria, evaluate the signal efficiency, and estimate background contributions.

Inclusive MC simulation samples are generated at different center-of-mass energies to study potential background reactions. These samples consist of open charm processes, the ISR production of vector charmonium and charmonium-like states, and the known hadronic continuum processes incorporated in KKMC [24, 25]. The known decay modes are modeled with EVTGEN [26, 27] using branching fractions taken from the Particle Data Group (PDG) [28], and the remaining unknown decays of the charmonium states are simulated with LUNDCHARM [29, 30]. Final-state radiation from charged final-state particles is incorporated with PHOTOS [31]. The signal MC simulation sample of $e^+e^- \to p p\bar{p}\bar{n}\pi^-$ at each energy point is generated with the events being uniformly distributed in phase space.

III. DATA ANALYSIS

Events with two positive and two negative charged tracks are selected. For each charged track, the polar angle in the MDC with respect to the z direction must satisfy $|\cos\theta| < 0.93$. All charged tracks are required to originate from the interaction region, defined as $R_{xy} < 1$ cm and $|V_z| < 10$ cm, where R_{xy} and $|V_z|$ are the distances from the point of closest approach of the tracks to the interaction point in the $x-y$ plane and in the z direction, respectively. The combined dE/dx and TOF information are used to calculate particle identification (PID) confidence levels for the pion, kaon, and proton hypotheses. Each track is assigned as the particle hypothesis with the highest confidence level. The final state in the $e^+e^- \to p p\bar{p}\bar{n}\pi^-$ process is reconstructed with two protons, one antiproton and one π^-. In this paper, charge conjugated process is implied.

Since the neutron can not be well reconstructed with the BESIII detector, the signal process is determined via the recoiling mass of the reconstructed charged particles, defined as

$$M_{\rm rec}c^2 = \sqrt{(E_{e^+e^-} - E_{pp\bar{p}\pi^-})^2 - (\vec{P}_{e^+e^-} - \vec{P}_{pp\bar{p}\pi^-})^2 \cdot c^2}, \quad (1)$$

where $E_{e^+e^-}$ and $\vec{P}_{e^+e^-}$ are the center-of-mass energy and the momentum of the e^+e^- system, respectively; $E_{pp\bar{p}\pi^-}$ and $\vec{P}_{pp\bar{p}\pi^-}$ are the total reconstructed energy and total momentum of the $pp\bar{p}\pi^-$ system, respectively. Events with $M_{\rm rec}$ greater than 0.8 GeV/c^2 are kept for further analysis.

Studies based on the inclusive MC simulation samples [32] show that no peaking background events survive the selection criteria. To further suppress background events, two additional selection criteria are imposed on the accepted candidate events. First, the invariant mass $M_{p\pi^-}$ of the reconstructed $p\pi^-$ system is required to be outside the Λ signal region, *i.e.* $|M_{p\pi^-} - 1.115| > 0.010$ GeV/c^2, to remove the possible background associated with Λ decays. Here, 1.115 GeV/c^2 is the known Λ mass [33], and 0.010 GeV/c^2 corresponds to about three times the mass resolution. Second, the invariant mass of $pp\bar{p}$ ($M_{pp\bar{p}}$) must be less than 3.6 GeV/c^2 due to the remaining neutron and pion in the event.

The $M_{\rm rec}$ distribution of the accepted candidates after the above selection criteria from the combined data sets is displayed in Fig. 1, where a significant neutron signal is observed. The signal yield is determined by a maximum likelihood fit to this distribution. In the fit, the signal is represented by the luminosity weighted MC-simulated shape convolved with a Gaussian function and the remaining background is described by a linear function. From the fit, the signal yield is determined to be 123 ± 14.

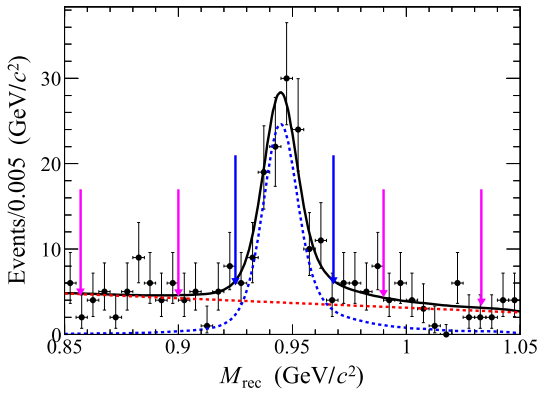

Fig. 1. (color online) Distribution of the recoiling mass $M_{\rm rec}$ of the candidate events for the reaction $e^+e^- \to p p\bar{p}\bar{n}\pi^-$ with the fit results overlaid. The dots with error bars are from the combined data sets, the black curve shows the total fit result, and the dashed blue (red) curve represents the signal (background) shape. The pair of blue arrows marks the neutron signal region, whereas the neutron sideband regions are visualized by the two pairs of pink arrows.

The statistical significance of the signal is determined to be 11.5σ, which is evaluated as $\sqrt{-2\ln(\mathcal{L}_0/\mathcal{L}_{\rm max})}$, where $\mathcal{L}_{\rm max}$ is the maximum likelihood of the nominal fit and $\mathcal{L}_0$ is the likelihood of the fit without involving the signal component. The change of the degree of freedom is 1. The neutron signal region is defined as $M_{\rm rec} \in (0.925, 0.968)$ GeV/c^2 and the corresponding sideband regions are defined as $M_{\rm rec} \in (0.857, 0.900) \cup (0.990, 1.033)$ GeV/c^2.

Figure 2 shows the comparisons of the momentum and polar angle distributions of the neutron of the accepted candidate events between data and signal MC simulation samples, where the data distribution is from the combined data sets and the MC simulation distribution has been weighted by the signal yields in data. The invariant mass of any two or three particles, the momentum and $\cos\theta$ distributions of the other final state particles have also been examined. The agreement between data and MC simulation allows to determine the detection efficiency with the signal MC simulation events generated uniformly distributed in the five-body phase space.

To search for hexaquark and di-baryon states, the $\bar{p}\bar{n}$ invariant mass spectrum is examined. Figure 3 shows the $pp\pi^-$ and $\bar{p}\bar{n}$ invariant mass spectra of the candidate events for the reaction $e^+e^- \to p p\bar{p}\bar{n}\pi^-$. In the fit to $M_{\bar{p}\bar{n}}$, the signal is represented by the luminosity weighted phase space MC simulation shape and the remaining combinatorial background is described by a linear function. The goodness-of-fit is $\chi^2/ndf = 38.21/37$. Here, ndf is the number of degrees of freedom. Compared to the phase space hypothesis, no obvious structure is observed.

IV. AVERAGE CROSS SECTIONS

In a data set for each energy point, only a few events have been observed in the neutron signal region, with a statistical significance of less than 3σ. To obtain significant neutron signals the data sets are combined into three sub-samples in the energy ranges of (4.160, 4.380), (4.400, 4.600) and (4.610, 4.700) GeV for further analysis.

The average observed cross section for $e^+e^- \to p p\bar{p}\bar{n}\pi^-$ is calculated by

$$\overline{\sigma}_j^{\rm obs} = \frac{N_j^{\rm sig}}{\Sigma_i \epsilon_{ji} \cdot \mathcal{L}_{ji}}, \tag{2}$$

where $N_j^{\rm sig}$ is the number of signal events from the j-th combined data set, $\mathcal{L}_i$ and ϵ_i are the integrated luminosity and efficiency of data set i, respectively, i represents the i-th energy point in j-th combined data set. The detection efficiency is corrected by correction factors for the PID and tracking efficiencies, $f_{\rm PID}$ and $f_{\rm trk}$, which are determined to be 0.92 and 0.98 by weighting the differences between efficiency experimentally determined and that in the MC simulation in different momentum ranges, respectively. Inserting the numbers which are listed in Table 1 into Eq. (2) yields the average observed cross sections $(19.4 \pm 5.1 \pm 1.0)$ fb, $(42.8 \pm 9.8 \pm 2.3)$ fb and $(54.2 \pm 8.6 \pm 2.9)$ fb for the three combined data sets, respectively, where the first uncertainties are statistical and the second are systematic.

To measure the average Born cross section of $e^+e^- \to p p\bar{p}\bar{n}\pi^-$, a similar lineshape as that of $e^+e^- \to 2(p\bar{p})$ [12] is assumed to determine the ISR and vacuum polarization correction factors, $(1+\delta^\gamma)$ and $\frac{1}{|1-\Pi|^2}$, as they are similar reactions where one of the $\bar{p}$ has been exchanged by $\bar{n}\pi^-$. The lineshape is constructed as

$$\sigma^{\rm Born}(s) = \frac{1}{s} \times e^{p_0(\sqrt{s}-M_{\rm th})} \times p_1, \tag{3}$$

where p_0 and p_1 are free parameters, $M_{\rm th} = (3m_p + m_n + m_{\pi^-})$, m_p, m_n, and m_{π^-} are the known masses of p, n, and π^- taken from the PDG [33]. The average Born cross sec-

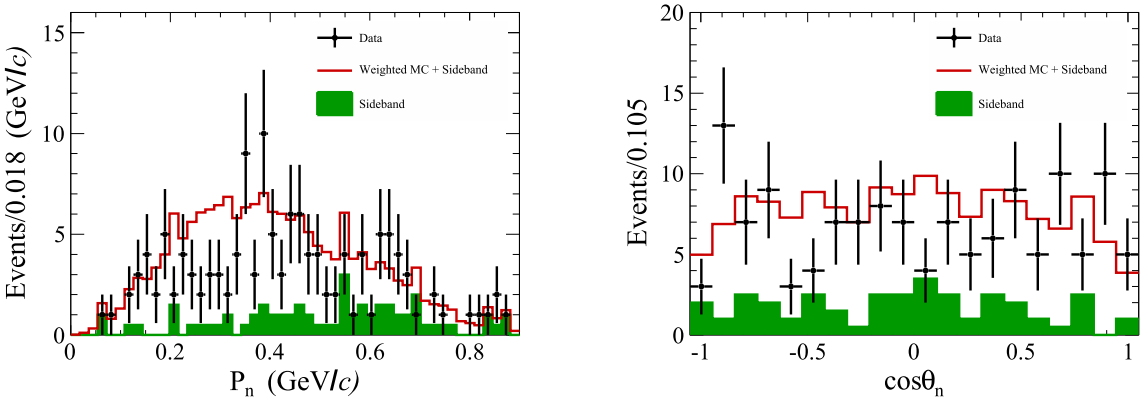

Fig. 2. (color online) Momentum (left) and polar angular distributions (right) of the neutrons of the candidate events for the reaction $e^+e^- \to p p\bar{p}\bar{n}\pi^-$. The dots with error bars represent the combined data sets. The green histograms represent the sideband events. The red histograms represent the weighted signal MC simulation events plus the normalized neutron sideband regions in data.

Table 1. The average observed cross sections for the reaction $e^+e^- \to p\bar{p}\bar{n}\pi^- + c.c.$. Summary of the number of signal events ($N_{\rm sig}$), integrated luminosity ($\mathcal{L}$), detection efficiency (ϵ), radiative correction factors $(1+\delta^{\gamma})$, the average observed cross section ($\overline{\sigma}^{\rm obs}$) and average Born cross section ($\overline{\sigma}^{\rm Born}$) at different c.m. energies ($\sqrt{s}$). The uncertainties are statistical only.

$\sqrt{s}$ /GeV	$\mathcal{L}$ /pb^{-1}	ϵ (%)	$(1+\delta^{\gamma})$	$N_{\rm sig}$	$\overline{\sigma}^{\rm obs}$/fb	$\overline{\sigma}^{\rm Born}$/fb
4.1574	408.70	4.2	0.8408			
4.1780	3189.0	6.0	0.8388			
4.1889	526.70	7.1	0.8430			
4.1990	526.00	8.1	0.8456			
4.2092	517.10	8.8	0.8485			
4.2188	514.60	9.6	0.8509			
4.2263	1056.40	10.1	0.8489			
4.2358	530.30	11.4	0.8530			
4.2439	538.10	12.0	0.8552	22.7 ± 6.0	19.4 ± 5.1	21.5 ± 5.7
4.2580	828.40	13.5	0.8559			
4.2668	531.10	14.0	0.8587			
4.2777	175.70	14.8	0.8593			
4.2878	502.40	14.2	0.8612			
4.3121	501.20	16.2	0.8628			
4.3374	505.00	18.6	0.8646			
4.3583	543.90	21.8	0.8693			
4.3774	522.70	21.0	0.8668			
4.3965	507.80	22.6	0.8674			
4.4156	1043.90	24.8	0.8764			
4.4362	569.90	25.0	0.8683	30.9 ± 7.1	42.8 ± 9.8	46.3 ± 10.6
4.4671	111.09	27.4	0.8794			
4.5271	112.12	30.7	0.8838			
4.5995	586.90	34.0	0.8876			
4.6152	103.83	33.5	0.8712			
4.6304	521.52	34.1	0.8710			
4.6431	552.41	34.5	0.8708	69.4 ± 11.0	54.2 ± 8.6	59.0 ± 9.4
4.6639	529.63	35.7	0.8712			
4.6842	1669.31	36.3	0.8711			
4.7008	536.45	36.6	0.8710			

tion is calculated by

$$\overline{\sigma}_j^{\rm Born} = \frac{\overline{\sigma}_j^{\rm obs}}{(1+\delta^{\gamma})_j \cdot \left(\frac{1}{|1-\Pi|^2}\right)_j}. \quad (4)$$

The obtained Born cross sections are then used as input in the generator and the cross section measurements are iterated with the updated detection efficiencies. This process is repeated until the $(1+\delta^{\gamma})\cdot\epsilon$ values become stable at all energies, *i.e.* the difference of $(1+\delta^{\gamma})\cdot\epsilon$ between the last two iterations is less than 4%. Figure 4 shows the obtained average Born cross sections in the defined subsamples. The average Born observed cross sections are calculated with Eq. (4), and the results are $(21.5\pm5.7\pm1.2)$ fb, $(46.3\pm10.6\pm2.5)$ fb and $(59.0\pm9.4\pm3.2)$ fb for the three combined data sets, respectively, where the first uncertainties are statistical and the second are systematic. Two different functions are used to compare the trend of the average Born cross section to a reaction where a similar behaviour is expected. The first one is a simple five-body energy-dependent phase space lineshape [12, 34] and the second one is an exponential function [12, 35], which are shown in Fig. 4. However, it should be noted that the two functions in Fig. 4 are not fit results, but drawn with arbitrary scale factors for comparison since a qualitative fit is not possible due to the limited statistics.

The systematic uncertainties in the cross section measurements will be discussed in the next section.

V. SYSTEMATIC UNCERTAINTY

In the cross section measurements, the systematic uncertainties mainly comes from the integrated luminosity, tracking efficiency, PID efficiency, ISR correction, $M_{\rm rec}$ fit, and veto of background events associated with Λ decays.

The integrated luminosity of the data set is measured by large-angle Bhabha scattering events, and the uncertainty in the measurement is 1.0% [21], which is dominated by the precision of the MC generator used for efficiency correction. The tracking and PID efficiencies have been studied with high purity control samples of $J/\psi \to p\bar{p}\pi^+\pi^-$ and $\psi(3686) \to \pi^+\pi^- J/\psi \to \pi^+\pi^- p\bar{p}$ decays [36, 37]. The differences of the tracking and PID efficiencies between data and MC simulation in different transverse momentum and total momentum ranges are obtained separately. The averaged differences for the tracking (PID) efficiencies are corrected by the factors $f_{\rm trk}$ ($f_{\rm PID}$) as mentioned in Sec. IV. The uncertainties of the tracking and PID efficiencies are reweighted by the $p/\bar{p}$ and π^+/π^- momenta of the signal MC simulation events. The reweighted uncertainties for tracking (PID) efficiencies, 0.1% (0.3%) per p, 0.1% (0.4%) per $\bar{p}$, 1.0% (0.5%) per π^+ and 0.8% (0.4%) per π^-, are assigned as the systematic uncertainties. Adding them linearly gives the total systematic uncertainties due to the tracking and PID efficiencies to be 1.1% and 1.6% for the process $e^+e^- \to p\bar{p}\bar{n}\pi^-$, and 1.3% and 1.9% for the process $e^+e^- \to p\bar{p}\bar{p}n\pi^+$, respectively.

The input Born cross sections in the generator are iterated until the $(1+\delta^{\gamma})\cdot\epsilon$ values converge. The largest difference of $(1+\delta^{\gamma})\cdot\epsilon$ between the last two iterations at

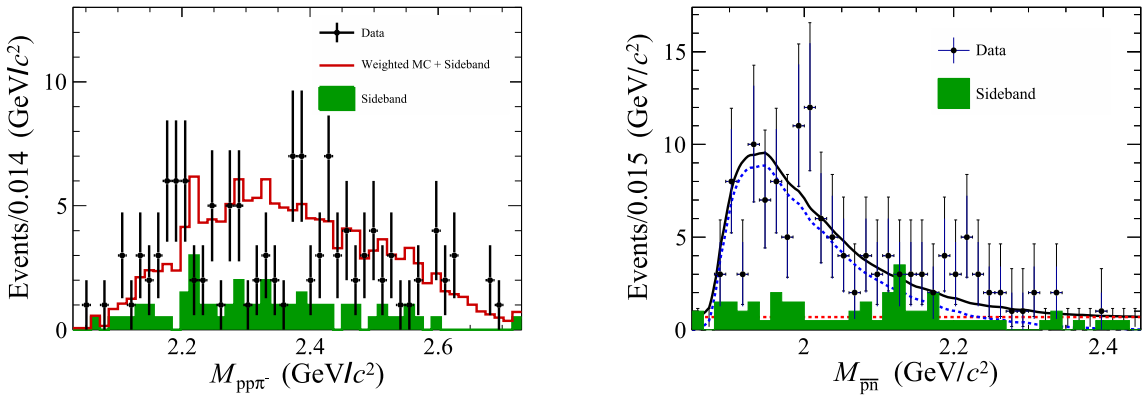

Fig. 3. (color online) The $p\pi^-$ (left) and $\bar{p}n$ (right) invariant mass spectra of the candidate events for $e^+e^- \to p p\bar{p}\bar{n}\pi^-$. The dots with error bars represent the combined data sets. The green histograms are the normalized neutron sideband events in data. The red histogram represents the weighted signal MC simulation events plus the normalized neutron sideband events in data. The black solid curve shows the total fit result, the blue dashed curve is the signal shape derived from the signal MC simulation sample, and the red dashed line is the linear background shape.

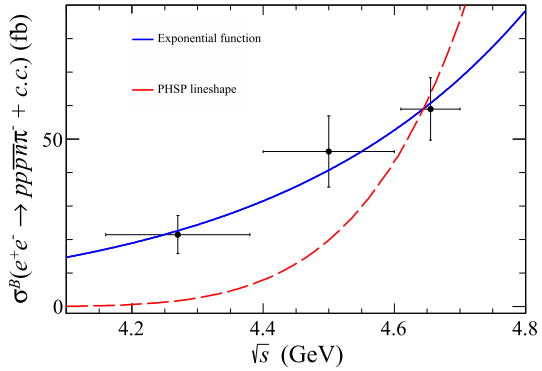

Fig. 4. (color online) Average Born cross sections for the process $e^+e^- \to p p\bar{p}\bar{n}\pi^- + c.c.$. The dots with error bars are the measured values, the blue line shows the exponential function curve and the red-dashed line shows the five-body energy-dependent phase spase (PHSP) lineshape curve.

all energy points, 3.2%, is taken as the corresponding systematic uncertainty.

Three different tests were performed to estimate the uncertainty associated with the $M_{\rm rec}$ fit. The fit range is increased or decreased by 5 MeV/c^2. The background shape is replaced with a second-order Chebychev polynomial function, and the signal shape is replaced with an MC simulation-derived shape. The quadrature sum of these changes, 3.6%, is taken as the relevant uncertainty.

The systematic uncertainty due to the veto of Λ background events is estimated by changing the Λ veto mass window from $\pm 3\sigma$ to $\pm 5\sigma$, where σ is the invariant mass resolution and the value is 3 MeV/c^2. The change of the measured cross section, 0.03%, is assigned as the uncertainty.

Adding the above systematic uncertainties summarized in Table 2 in quadrature yields the total systematic uncertainties of 5.3% and 5.4%, for the processes $e^+e^- \to p p\bar{p}\bar{n}\pi^-$ and $e^+e^- \to p\bar{p}\bar{p}n\pi^+$, respectively. The average systematic uncertainty, 5.35%, is taken as the total systematic uncertainty in the cross section measurement for the process $e^+e^- \to p p\bar{p}\bar{n}\pi^- + c.c.$.

Table 2. The relative systematic uncertainties (in %) from the integrated luminosity of data set ($\mathcal{L}$), the tracking efficiency (Trk), the PID efficiency (PID), the ISR correction (ISR), the $M_{\rm rec}$ fit (Fit), and the Λ veto in the cross section measurements.

Mode	$\mathcal{L}$	Trk	PID	ISR	Fit	Λ veto	Total
$p p\bar{p}\bar{n}\pi^-$	1.0	1.1	1.6	3.2	3.6	0.03	5.3
$p\bar{p}\bar{p}n\pi^+$	1.0	1.3	1.9	3.2	3.6	0.03	5.4

VI. SUMMARY

By using the data sets taken at the center-of-mass energies between 4.16 and 4.70 GeV, the process $e^+e^- \to p p\bar{p}\bar{n}\pi^- + c.c.$ has been observed for the first time with a statistical significance of 11.5σ. The average Born cross sections in the three energy ranges of (4.160, 4.380), (4.400, 4.600) and (4.610, 4.700) GeV are measured to be $(21.5 \pm 5.7 \pm 1.2)$ fb, $(46.3 \pm 10.6 \pm 2.5)$ fb and $(59.0 \pm 9.4 \pm 3.2)$ fb, respectively, where the first uncertainties are statistical and the second systematic. The shape of the invariant-mass spectra of $\bar{p}n$ and $p\pi^-$ are in good agreement with the phase-space distributions, thereby indicating no hexaquark or di-baryon state observed with the current data sample size.

ACKNOWLEDGMENTS

The BESIII collaboration thanks the staff of BEPCII and the IHEP computing center for their strong support.

References

[1] E. Braaten, C. Langmack, and D. Hudson Smith, Phys. Rev. D **90**, 014044 (2014)
[2] C. J. Morningstar and M. J. Peardon, Phys. Rev. D **60**, 034509 (1999)
[3] M. Ablikim *et al*. (BESIII Collaboration), Phys. Rev. Lett. **110**, 252001 (2013)
[4] R. Aaij *et al*. (LHCb Collaboration), Phys. Rev. Lett. **115**, 072001 (2015)
[5] S. M. Gerasyuta and E. E. Matskevich, Phys. Rev. D **106**, 114028 (2022)
[6] W. Park, A. Park, and S. H. Lee, Phys. Rev. D **92**, 014037 (2015)
[7] M. Bashkanov *et al*. (CELSIUS/WASA Collaboration), Phys. Rev. Lett. **102**, 052301 (2009)
[8] P. Adlarson *et al*. (WASA-at-COSY Collaboration), Phys. Rev. Lett. **106**, 242302 (2011)
[9] F. Kren *et al*. (CELSIUS/WASA Collaboration), Phys. Lett. B **684**, 110 (2011)
[10] P. Adlarson *et al*. (WASA-at-COSY Collaboration), Phys. Rev. C **88**, 055208 (2013)
[11] P. Adlarson *et al*. (WASA-at-COSY Collaboration), Phys. Lett. B **743**, 325 (2015)
[12] M. Ablikim *et al*. (BESIII Collaboration), Phys. Rev. D **103**, 052003 (2021)
[13] M. Ablikim *et al*. (BESIII Collaboration), Nucl. Instrum. Meth. A **614**, 345 (2010)
[14] C. H. Yu *et al.*, Proceedings of IPAC2016, Busan, Korea, 2016
[15] M. Ablikim *et al*. (BESIII Collaboration), Chin. Phys. C **44**, 040001 (2020)
[16] X. Li *et al*., Radiat. Detect. Technol. Methods **1**, 13 (2017)
[17] Y. X. Guo *et al*., Radiat. Detect. Technol. Methods **1**, 15 (2017)
[18] M. Ablikim *et al*. (BESIII Collaboration), Chin. Phys. C **40**, 063001 (2016)
[19] M. Ablikim *et al*. (BESIII Collaboration), Chin. Phys. C **45**, 103001 (2021)
[20] M. Ablikim *et al.* (BESIII Collaboration), Publication in preparation
[21] M. Ablikim *et al.* (BESIII Collaboration), Submitted to Chin. Phys. C, arXiv: 2203.03133[hep-ex]
[22] Z. Y. Deng *et al*., High Energy Physics & Nuclear Physics **30**, 371 (2006)
[23] S. Agostinelli *et al*. (GEANT4 Collaboration), Nucl. Instrum. Meth. A **506**, 250 (2003)
[24] S. Jadach, B. F. L. Ward, and Z. Was, Comput. Phys. Commun. **130**, 260 (2000)
[25] S. Jadach, B. F. L. Ward, and Z. Wąs, Phys. Rev. D **63**, 113009 (2001)
[26] R. G. Ping, Chin. Phys. C **32**, 599 (2008)
[27] D. J. Lange, Nucl. Instr. Meth. A **462**, 152 (2001)
[28] J. Beringer *et al.* (Particle Data Group), Phys. Rev. D **86**, 010001 (2012) and 2013 partial update for the 2014 edition
[29] J. C. Chen, G. S. Huang, X. R. Qi *et al*., Phys. Rev. D **62**, 034003 (2000)
[30] R. L. Yang, R. G. Ping, and D. Chen, Chin. Phys. Lett. **31**, 061301 (2014)
[31] E. Richter-Was, Phys. Lett. B **303**, 163 (1993)
[32] X. Y. Zhou, S. X. Du, G. Li *et al*., Comput. Phys. Commun. **258**, 107540 (2021)
[33] M. Tanabashi *et al*. (Particle Data Group), Prog. Theor. Exp. Phys. **2020**, 083C01 (2020)
[34] E. Byckling and K. Kajantie, *Particle Kinematics*, (Wiley, New York, 1973)
[35] M. Ablikim *et al*. (BESIII Collaboration), Phys. Rev. Lett. **118**, 092001 (2017)
[36] M. Ablikim *et al*. (BESIII Collaboration), Phys. Rev. D **91**, 112004 (2015)
[37] M. Ablikim *et al*. (BESIII Collaboration), Phys. Rev. D **99**, 031101 (2019)